4.2 CHARACTERISTICS OF ATMOSPHERIC AEROSOLS USING OPTICAL REMOTE SENSING

C. Russell Philbrick*, Timothy Wright, Michelle Snyder, Hans Hallen
North Carolina State University, Raleigh NC
Andrea M. Brown, Sachin Verghese, Perry S. Edwards
Penn State University, University Park, PA

1. INTRODUCTION

Laser remote sensing techniques now provide important tools for determining most of the properties of aerosols, including their physical and chemical characteristics. Examples are selected to show the types of information contained in the optical scattering signatures. Improvements in our understanding the distribution of aerosols, their sources, and processes controlling their formation and growth are needed for a detail understanding of their contributions to the planetary albedo and their influence on radiative transfer. These are critically important factors for developing accurate predictions of changes to be expected in our climate.

Multi-wavelength backscatter measurements from Rayleigh and Raman lidar techniques provide signals that are used to profile the properties that govern the transmission of radiation through an atmospheric column. Rayleigh lidar signals provide backscatter coefficients, and Raman lidar signals backscattered from the major molecular components provide extinction profiles. The ratio of these simultaneous extinction and backscatter measurements are used to describe the aerosol type. In addition, a laser beam can be used to make bistatic and multistatic measurements of the polarization ratio of the scattering phase function. Analysis of multistatic measurements can be used to determine profiles of the aerosol number density, size, size distribution, and type. These parameters can be measured for spherical particles in the size range between about 20 nm and 20 μm. Analysis of the size distribution requires adopting a mathematical function, which is usually taken to be a log-normal distribution. Information on aerosol type and shape can be supposed from determining the approximate refractive index of the scattering aerosols and by measuring the depolarization of the scattered radiation.

2. RAYLEIGH AND RAMAN SCATTERING

Rayleigh and Raman lidar measurements of scattering by molecules and aerosols provide the profiles of optical backscatter and extinction that determine the atmospheric optical properties influencing radiative transfer. DIAL lidar techniques, hyper-spectral sensors, developments of multi-wavelength lidar, and the recent supercontinuum techniques provide measurements of trace species needed to describe the optical absorption properties that also affect the radiation balance.

In the troposphere, the direct backscatter optical signals of laser beams from the mixture of molecules and aerosols provides only limited information on the atmospheric properties; primarily cloud ceiling, a profile of relative backscatter coefficient, and an indication of the presence of aerosol layers. However, Raman lidar can provide more valuable information, including profiles of all major molecular species (N_2, O_2, H_2O), several minor species (O_3, CO_2), temperature from rotational Raman scattering, dynamical processes from tracers such as water vapor, and aerosol extinction from the gradients in the vertical profiles of the molecular constituents (OBrien et al. 1996, Philbrick 2002, Li and Philbrick 2002, Philbrick 2005). Analyzing the gradients in the vertical profiles of the vibrational Raman signals of N_2, O_2, and the rotational Raman molecular signals, and comparing them with the expected hydrostatic profile of the molecular atmosphere provides robust profiles of the optical extinction at several wavelengths, see Fig. 1. The profile of the molecular atmosphere can be obtained using the measured rotational Raman temperature profile. As expected, the profiles of different wavelengths all approach the same value as multiple scattering properties begin to dominate (note the layer at 4.5 km). Extinction profiles for several wavelengths are quite useful for observing changes in the particle size, as a function of altitude and time. In the case of shown in Fig. 1, where different wavelengths are used (250-600 nm), we observe changes in time and space of the accumulation mode particles.

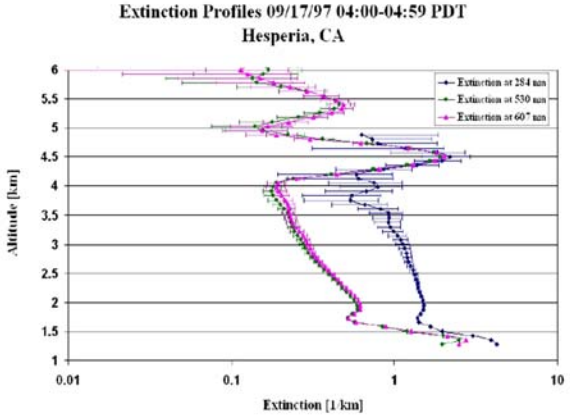

Figure 1. Vertical extinction profiles from vibrational Raman profiles of N_2 at 284 and 607 nm, and rotational Raman profiles of the integrated molecular species scattering in a band at 530 nm are shown (Verghese et al. 2005, Philbrick 2005).

*Corresponding author address: Prof. Russell Philbrick, NC State University, MEAS Department, Raleigh, NC 27695-8208; email: philbrick@ncsu.edu.

Comparison of the ultraviolet and visible wavelength extinction profiles as a function of time in Fig. 2 shows the evolution of cloud development. Figure 3 shows the water vapor and the optical extinction during the early development of a cloud, which in these initial stages is sub-visual. The evolution in a developing cloud is first detected as an increase in the water vapor concentration, then the aerosols are detected as ultraviolet extinction, and later as extinction at visible wavelengths. Figure 4 presents a time sequence of optical extinction for the ultraviolet and visible wavelengths. Notice the more extensive regions of scattering by smaller particles observed in the shorter wavelength (UV) plot. The values become comparable within the cloud where multiple scattering dominates as observed in Fig. 1. The simultaneous measurements of water vapor and temperature shown in left panels of Figure 5 are used to calculate the relative humidity shown in the upper right panel. Comparisons of the measurements of optical extinction shown in the lower right panel with the relative humidity demonstrate the relationship between the aerosols occurrence in regions of higher humidity.

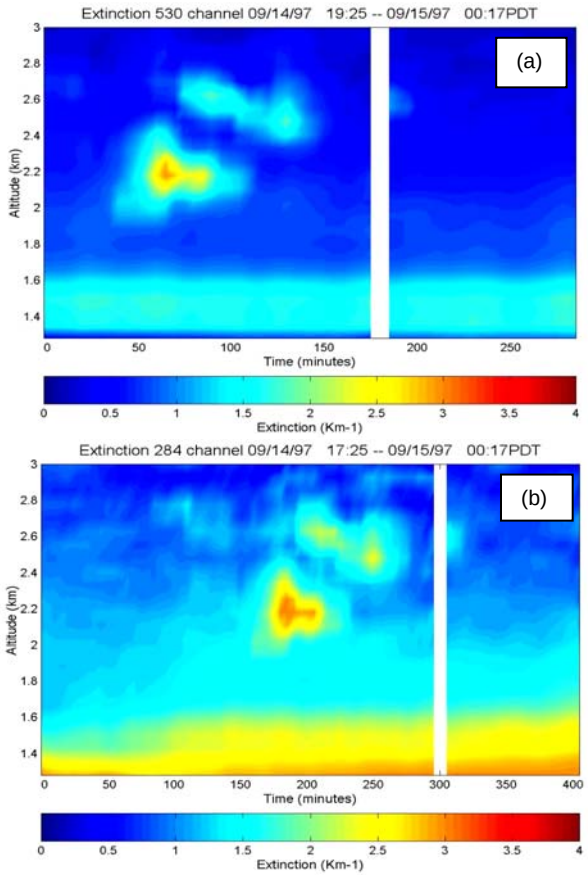

Figure 2. A time sequence of optical extinction profiles shows the development of a cloud moving through the vertical lidar beam; (a) visible (530 nm), (b) ultraviolet (284 nm). These measurement were made during the SCOS97 study at Hisperia CA at an elevation of 1.2 km (Verghese et al. 2005).

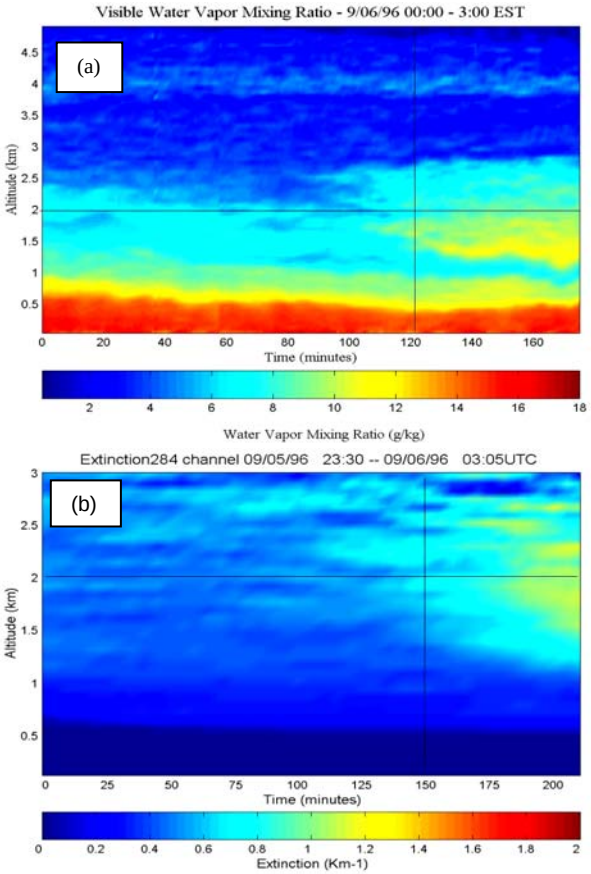

Figure 3. Time sequences of water vapor profiles (a) indicate the development of a cloud before it shows up in the UV extinction (b) (lines assist in locating corresponding points).

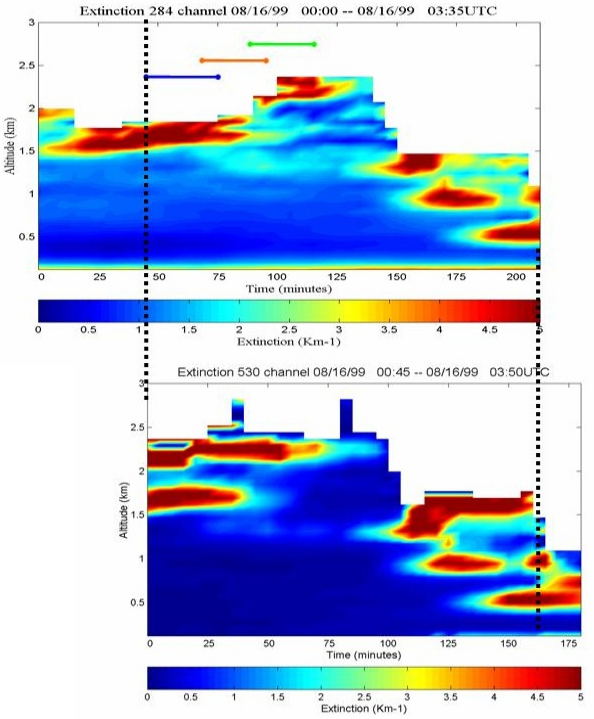

Figure 4. Time sequence cloud scattering, UV (284 nm) VIS (530 nm), (Verghese et al 2005, Verghese 2008).

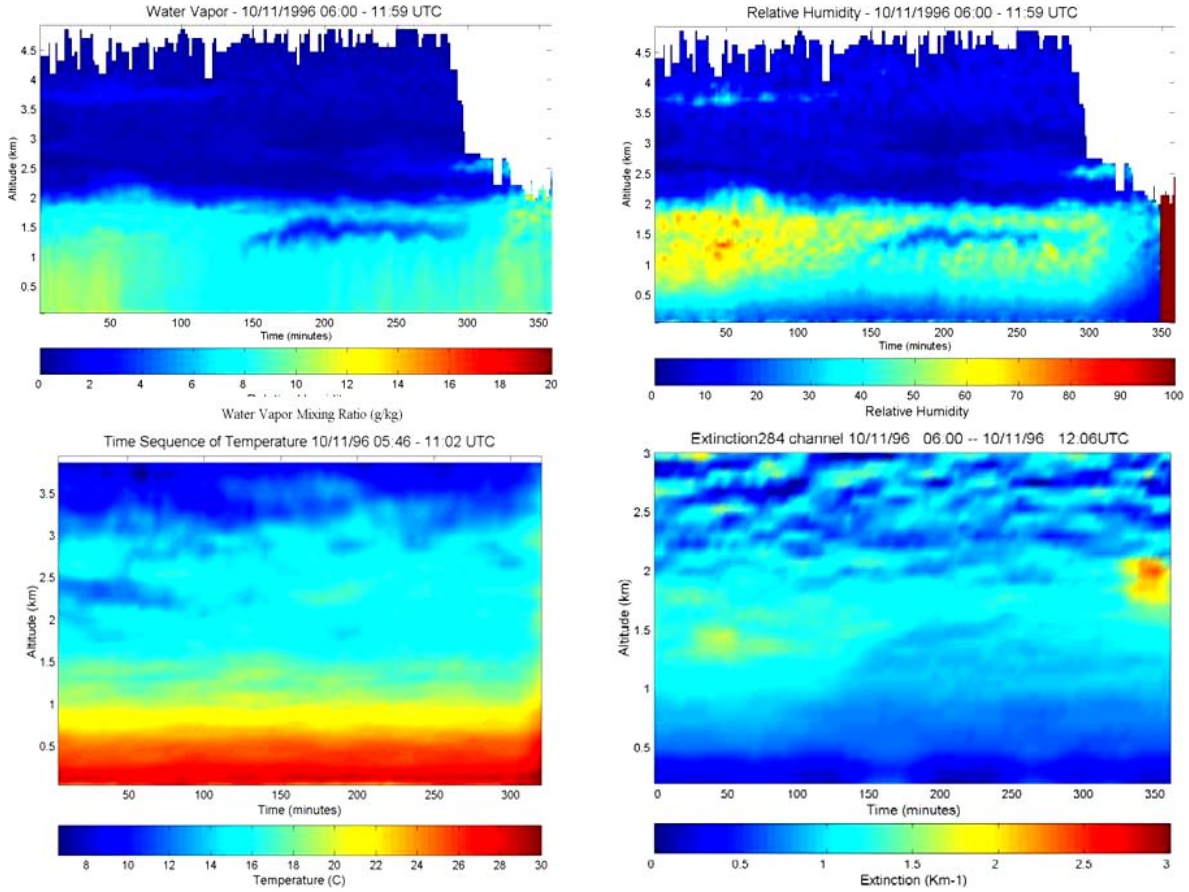

Figure 5. The parameters measured by the Raman lidar, water vapor and temperature (left side) are used to calculate the relative humidity, and this can be compared with the measured extinction to examine the regions of haze and cloud formation (Philbrick 2005).

3. AEROSOL OPTICAL SCATTERING

We have shown above that the optical extinction profiles can be obtained directly from the Raman lidar profile measurements of the primary molecular constituents; additionally information on the changes in particle size can be inferred. The same laser beam that is used for the vertical or horizontal Raman lidar measurements can be bistatic imaged to analyze the scattering phase function and determine more details regarding the aerosol properties. Figure 6 shows four cases where the angular intensity of the scattered radiation increases and the pattern becomes more complex as the ratio of the particle size to the wavelength increases. The scattering phase function of each polarization of the incident light (perpendicular or parallel with the plane containing the beam and the imaging device) can be measured from digital images of the beam. Figures 7, 8, 9, and 10 show results from a series of tests designed to demonstrate this capability by using bistatic lidar measurements to describe aerosol properties. Investigations using the intensity of the scattering to study aerosol properties was examined earlier (Reagan et al 1982a, 1982b); however, these more recent investigations are making use of the imaging information contained in the polarization ratio of the scattering phase function to eliminate uncertainties from the extinction along paths to the imaging detectors.

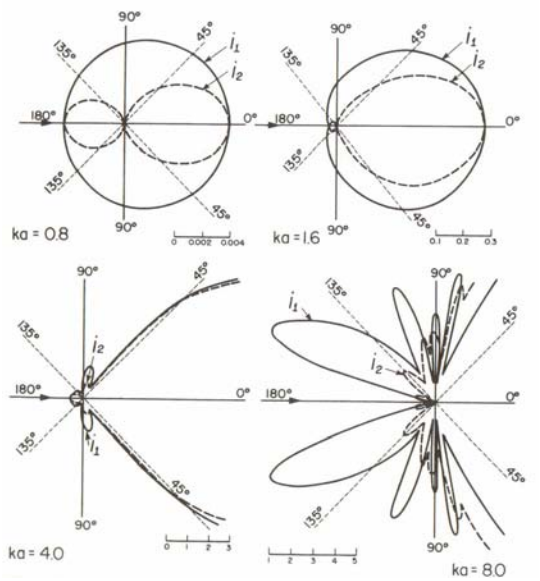

Figure 6. The angular variation of the intensity of the scattering phase function is shown for both polarizations and several cases of $k = 2\pi a/\lambda$ (a is the particle size and λ is the scattering wavelength (Born and Wolf, 2002).

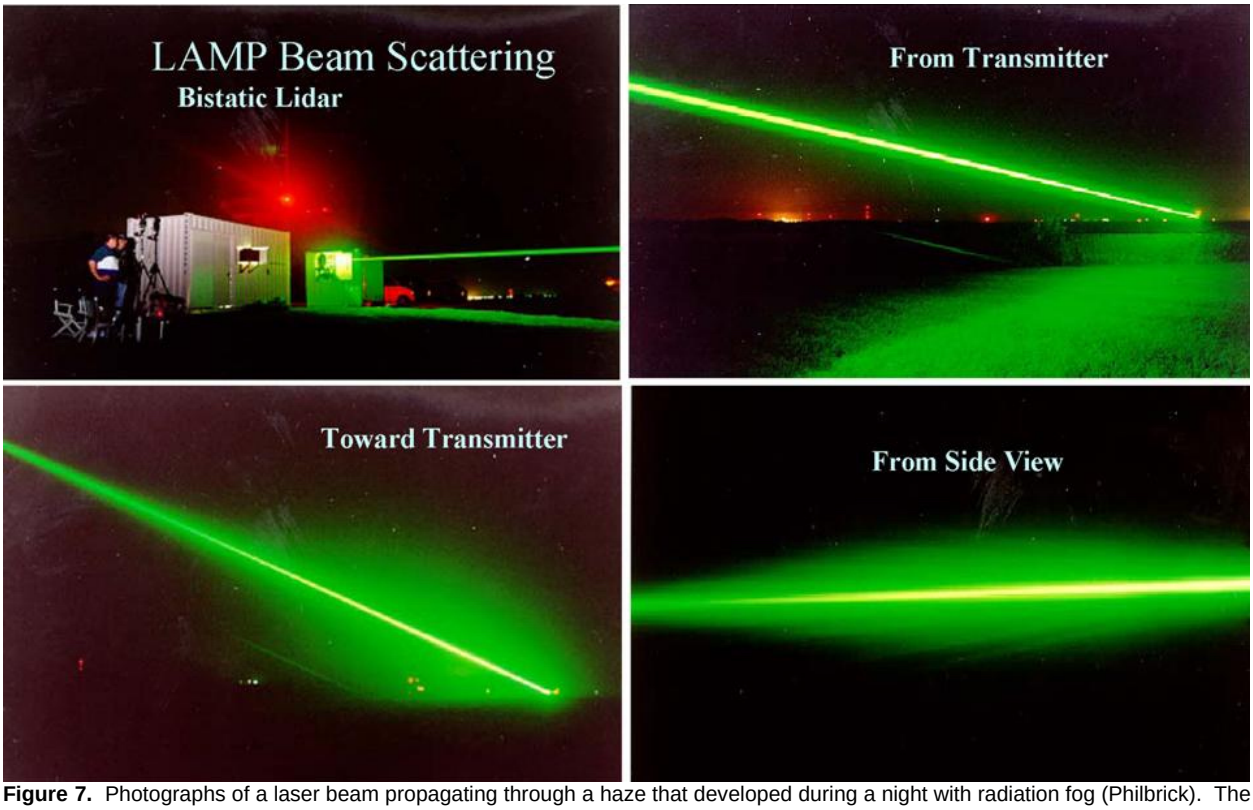

Figure 7. Photographs of a laser beam propagating through a haze that developed during a night with radiation fog (Philbrick). The views of the arrangement, see Fig.7, looking along the beam, back toward the transmitter, and from the side show the classic intensity distributions from the scattered intensity.

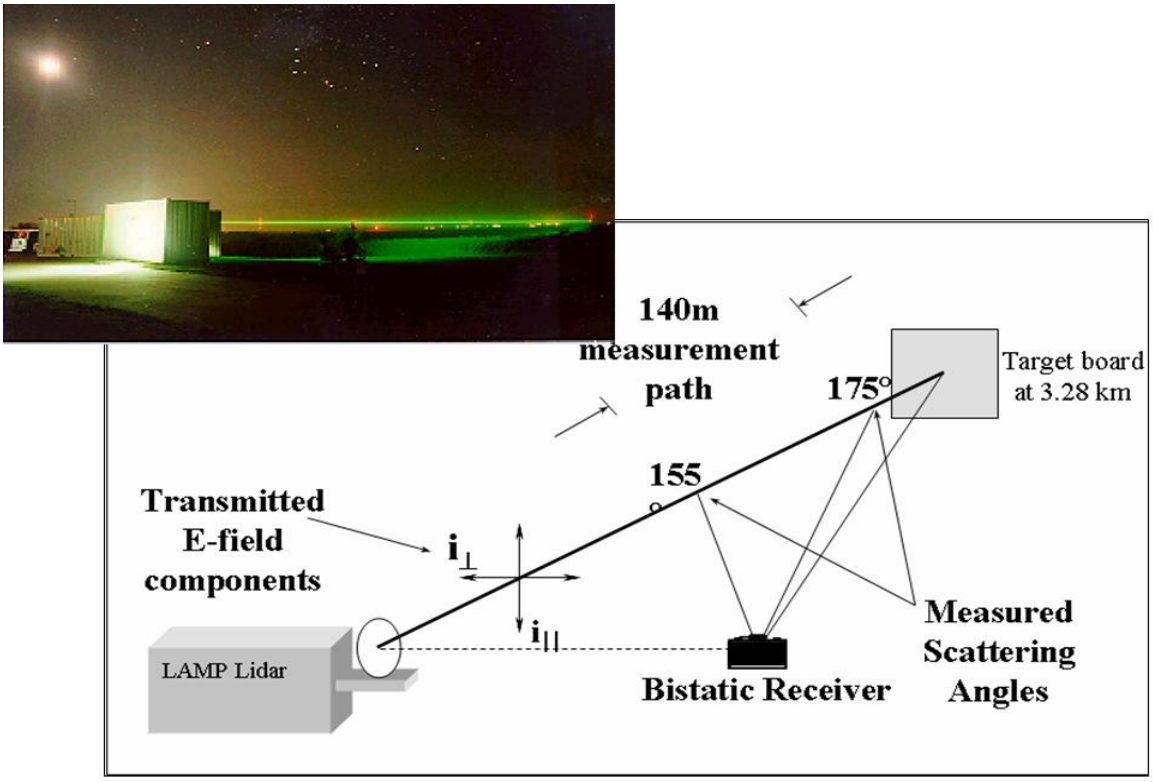

Figure 8. The arrangement for the bistatic lidar measurements during the CASES project at NASA Wallops in September 1995. The measurements were made using the LAMP Raman lidar which measured optical extinction on the path (Stevens et al. 1996).

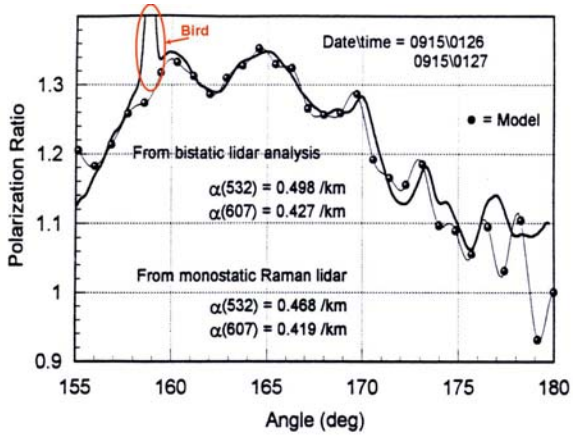

Figure 9. Polarization ratio from the measured intensities is compared with calculations from the best fit solutions of the Mie equations. The solution is shown in Fig. 9 (Stevens and Philbrick 1996a and 1996b, Stevens 1996).

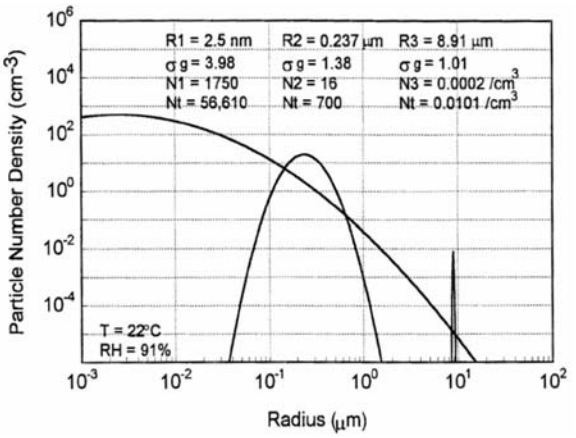

Figure 10. The analysis of data shown in Fig.8 resulted in a process for fitting these tri-modal distributions to determine the density and size (peak and distribution width) for the aerosols -- the peak at 9 μm contributes most to scattering (Stevens and Philbrick 1996a and 1996b, Stevens 1996).

Our approach for most bistatic measurements is to make use of the high power Raman lidar beam. Research campaigns have used horizontal paths with end-points on hard targets, like the one shown in Fig. 8, and vertical measurements using several receivers to resolve layered structures. Vertical measurements of the Raman lidar provide an ideal configuration for making multi-static measurements of the aerosol properties. It was found that vertical measurements require simultaneous data at two or more angles to resolve the aerosol properties. The system uses imaging detectors to measure the intensity as a function of angle, and the detectors are placed along radials on the planes of the parallel and perpendicular polarization of the laser transmitter. If one radial is used, the polarization plane can be flipped 90° by inserting a polarization rotator. Measurements of the two components of polarization are normally obtained within a period of a few seconds (optical shutter times are a fraction to a couple of seconds), and fresh data sets are typically obtained about once per minute.

An example from the bistatic measurements from the CASES experiment is shown in Fig. 9 and 10. In Fig. 9, the polarization ratio formed from the intensities of each pixel of the imaging array is plotted versus angle. The data for angles near 180° does not contain significant information. The analysis uses an array calculated from the Mie equations of aerosol scattering for spherical particles to find the best match for a tri-modal distribution of particles. The free parameters to be fit are the size and distribution of sizes, and the number densities for the three modes. In addition to the assumption of spherical particles, an assumption for the size distribution function is necessary; we have selected the log-normal distribution. Another parameter that can be estimated from the analysis is the index of refraction. Figure 10 shows the solution for data in Fig. 9. The result of integrated extinction caused by the scattering particles can be calculated for any wavelength. The optical extinction values at 532 and 607 nm corresponding to the solution in Fig. 10 are shown in the inset of Fig. 9; also shown are the values obtained from the Raman lidar measurements. The extinction values differ by about 5% and are within the measurement errors.

The development of the vertical profile analysis showed the approach to resolve the profiles of the vertical structure of aerosol layers. The key to obtaining accurate results is to over-determine the solution by making measurements at several different angles simultaneously in overlapping the field-of-view (fov) from several imagers; four or five locations along the radial are preferred. The angles can be determined accurately in the case when the end-point of the vertical beam is contained in the fov; also the star field can be imaged at night. The imagers are fitted with band filters for the laser wavelength (532 nm was used in this case), but the bandwidth cannot be narrow or the angular acceptance is too small. Future configurations will make use of confocal optics to allow use of narrow band filters and permit measurements in higher backgrounds.

4. SATELLITE REMOTE SENSING OF AEROSOLS

Multistatic lidar measurements of aerosol backscatter have proven quite useful for studying aerosols. We have also examined the forward scatter angles, which do not contain as much detail; however, the same properties can be obtained. We have proposed the idea of using measurements of a ground based laser from a satellite. This approach could provide an important data base on the aerosol optical properties. The cost of putting a laser in space caused our attention to focus on using a number of ground based laser/lidar systems combined with a satellite receiver to provide a unique approach for studying the complex atmospheric optical properties. Figures 11-14 show the basic concept.

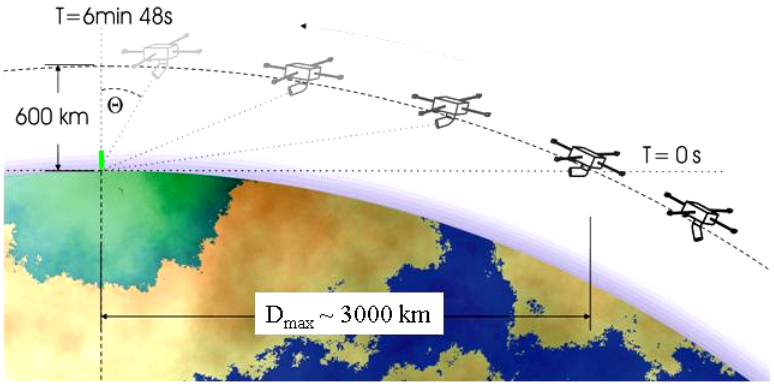

Figure 11. A schematic representation of the concept of using a vertical lidar, a laser step-pointed at a few locations along the satellite track, and low-power multi-λ diode lasers pointed at the satellite to record the atmospheric optical properties (Philbrick and Hallen,2009).

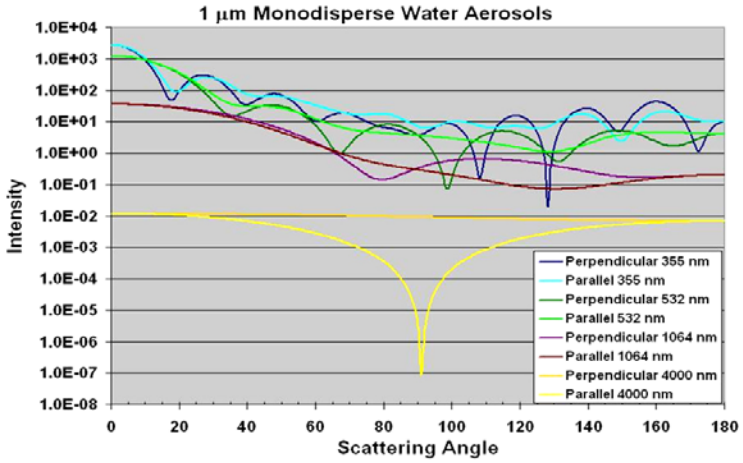

Figure 12. The angular distribution of the scattering intensity parallel and perpendicular to the laser polarization for 1 μm mono-dispersed aerosols when illuminated with 355, 532, 1064, and 4000 nm wavelengths (Philbrick and Hallen,2009).

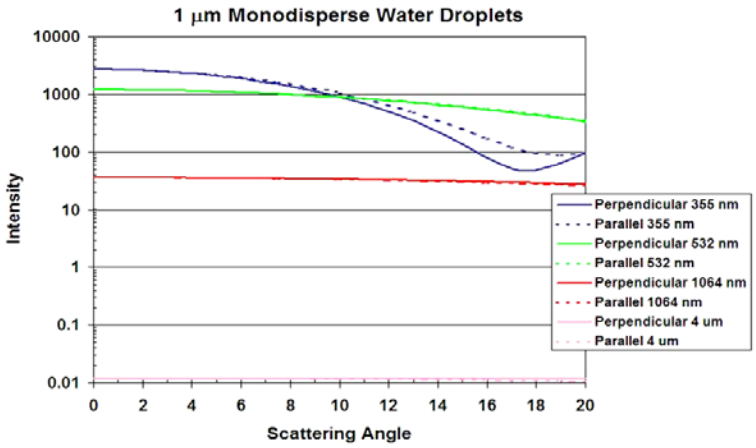

Figure 13. The scattering intensity shown in Fig. 11 for the 0-20^{o} region is enlarged of 1 μm particles (Philbrick and Hallen,2009).

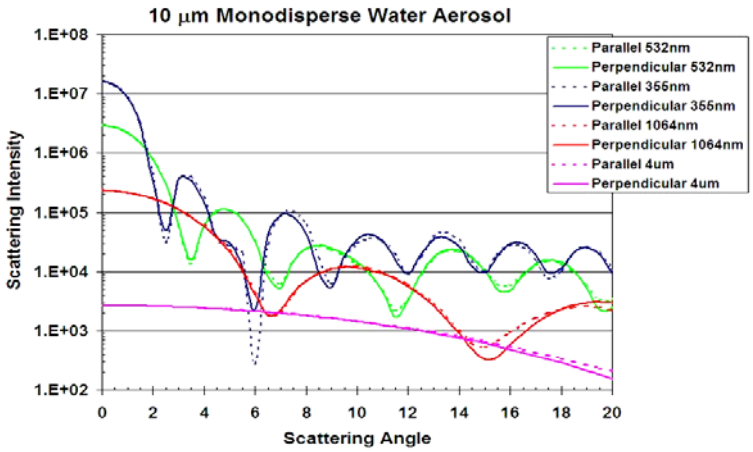

Figure 14. The forward scattering intensity for 10 mm aerosols can be compared with Fig. 11 and 12 to see the change in information contained in the signal. In practice, the signature is due to a distribution of particle sizes and often includes more than one mode (Philbrick and Hallen,2009).

The aerosol experiment uses the angular distribution of the scattered intensity, the polarization phase function measurements, and the path extinction at four wavelengths (355, 532, 1064, 4000 nm) to characterize aerosol properties. Scattering information is most useful when applied to a range of particle size versus wavelength values with ratio between 0.1 and 10. Thus, we expect the selected wavelengths are most useful for characterizing aerosols in the size range between 30 nm and 40 μm. Fig. 12 shows the scattering intensities in the back and forward scatter directions for a 500 nm light beam scattering from 1 μm spherical aerosol particles. Fig. 12 shows the intensity as a function of angle for the several wavelengths between UV and MWIR.

The calculations shown in Fig. 12 describe the full range of scattering angles for the case of 1 μm monodispersed water vapor aerosols. In Fig. 13, the scales are expanded to show the forward scatter intensity in the 0 to 20^{o} range for 1 μm aerosols and Fig. 14 shows 10 μm aerosols. In the case of satellite measurements, only the forward scattering intensity is measured. Of course the backscatter signal should be simultaneously measured at the ground level for analysis of the near-field aerosol properties. The approach is to point to a location on the orbit path about 15 to 20^{o} ahead of the satellite and make measurements as the satellite motion scans through the angles. After the satellite passes the nearest coincidence point, then the beam is repositioned to a location another 20 to 30^{o} ahead on the satellite path. This procedure should provide several independent path measurements during the satellite pass, and thus allow a measurement of spatial variations. Of course, the analysis must take into account the changing path and the fact that the aerosols are not mono-dispersed. We have been able to separate three simultaneously present aerosol size groups while using a single scattering wavelength, and expect that multiple wavelengths will over determine the situation to provide an accurate solution, even in the case of aerosol layers.

Aerosol measurements from satellites are difficult to interpret as evidenced from the fact that different groups have retrieved different aerosol properties from the same data because of different assumptions used in the analysis process. A 2007 workshop in Bremen, Germany has begun the process of addressing these problems (Kokhanovsky et al 2009). An additional problem that does not appear to have received sufficient attention is the difference in the processes for radiation transfer through different particle size distributions of aerosols. The radiative transfer is quite different through layers of 1 μm and 10 μm aerosols as is quickly evident from examining Fig. 13 and 14. Another factor which needs attention is the contribution of the sub-visual aerosols that are present at the edges of clouds, and in the regions where clouds are in their growth and dissipation phases. These small aerosols do participate in scattering of the short wavelength solar radiation; however, they are not detectable with currently used sensors and are not mapped as part of the cloud cover parameter. Haze layers are also difficult to measure, but their effect should be considered as a contribution to the overall radiative forcing. These factors, haze layers and edges of clouds, can be better observed and described by using the wavelength range and sensors described here.

The approach of using a number of ground-based laser transmitter sites that are co-located with the Raman lidar for standard meteorological measurements will result in a valuable data set. The implementation of this approach should provide a cost effective way to measure the optical, chemical, and aerosol scattering properties that are needed for the model and simulation developments. The measurements from space with a well defined reference source have major advantages compared with the hyper-spectral measurements, which rely on reflected sunlight. The complications associated

with convolving the variable optical backgrounds affecting source transmission into and through the atmosphere with the surface reflectance and the properties of the backscattered path to the satellite instrument require that several assumptions be made. The type of measurement parameters suggested here provide results that are more directly applicable and should be more useful for developing models and testing simulations used in climate change predictions.

A major advance in our use of the scattering information resulted from the work of Novitsky (2002 and Novitsky and Philbrick 2005), when he developed the multistatic lidar system. The technique has been extended to the case of aerosol multiple scattering and resulted in useful experimental and theoretical advances (Park and Philbrick 2006 and Park 2008). A solution for the full range of angles of scattering phase function for the case of multiple scattering is now available; previously, the region near 0^o and 180^o was available. The next advances are underway by making use of multi-wavelength scattering using several laser wavelengths simultaneously; even the case of using a supercontinuum laser is studied (Wyant et al 2009). The investigations of aerosols are being combined with measurements of other meteorological parameters from Raman lidar and from Differential Absorption Spectroscopy (DAS) to examine the optical properties through the optical spectrum (Philbrick et al 2009).

5. REFERENCES

Born, Max and Emil Wolf, Principles of Optics: Cambridge University Press, 40 West 20th Street, New York, NY, USA, 2002.

Kokhanovsky, Alexander and Gerrit de Leeuw, "Determination of Atmospheric Aerosol Properties Over Land Using Satellite Measurements," Bull. Am. Met. Soc. 90, 235-237, 2009.

Li, Guankun, and C. Russell Philbrick, "Lidar Measurements of Airborne Particulate Matter," in Remote Sensing of the Atmosphere, Environment, and Space, SPIE , 4893-15, 2002.

Novitsky, Edward J., PhD Dissertation, Department of Electrical Engineering, Penn State University, 2002.

Novitsky, E. J., and C.R. Philbrick, "Multistatic Lidar Profiling of Urban Atmospheric Aerosols," J. Geophy. Res. - Atmospheres, Vol. 110, DO7S11, 2005.

O'Brien, M.D. T. D. Stevens and C. R. Philbrick, "Optical Extinction from Raman Lidar Measurements," Optical Instruments for Weather Forecasting, SPIE Proc. Vol. 2832, 45-52, 1996.

Park, Jin H., and C. Russell Philbrick, "Multiple Scattering Measurements Using Multistatic Lidar," Proc. International Aerosol Conference, 2006.

Park, Jin H., PhD Dissertation, Department of Electrical Engineering, Penn State University, 2008.

Philbrick, C.R., "Raman Lidar Descriptions of Lower Atmosphere Processes," Lidar Remote Sensing in Atmospheric and Earth Sciences, Proc. 21st ILRC, Valcartier, Quebec Canada, 535-545, 2002.

Philbrick, C.R., "Raman Lidar Characterization of the Meteorological, Electromagnetic and Electro-optical Environment," Proc. SPIE Vol. 5887, Lidar Remote Sensing for Environmental Monitoring VI, p. 85-99, 2005.

Philbrick, C. Russell, David M. Brown, Adam H. Willitsford, Perry S. Edwards, Andrea M. Wyant, Zhiwen Z. Liu, C. Todd Chadwick, and Hans Hallen, "Remote Sensing of Chemical Species in the Atmosphere" *Proc. of Fourth Symposium on Lidar Atmospheric Applications*, as part of the 89th AMS Annual Meeting, Phoenix, Arizona, 11–15 Jan. 2009 http://ams.confex.com/ams/pdfpapers/150051.pdf

Philbrick, C. Russell, Hans Hallen, "Measurements of Contributors to Atmospheric Climate Change," Proc. 19th Symposium on European Rocket and Related Research, ESA Special Publication SP-671, 2009.

Reagan, J.A., D.M. Byrne and B.M. Herman, "Bistatic LIDAR: A Tool for Characterizing Atmospheric Particulates: Part I – The Remote Sensing Problem," IEEE Geosciences and Remote Sensing 20 229, 1982.

Reagan, J.A., D.M. Byrne and B.M. Herman, "Bistatic LIDAR: A Tool for Characterizing Atmospheric Particulates: Part II – The Inverse Problem," IEEE Geosciences and Remote Sensing 20 236, 1982.

Stevens, T.D., and C. R. Philbrick, "Particle Size Distributions and Extinction Determined by a Unique Bistatic Lidar Technique," Proceeding of IGARSS96 Conference on Remote Sensing for a Sustainable Future (International Geophysics and Remote Sensing Symposium) at Lincoln NB, May 1996, Vol II pg 1253-1256, 1996a.

Stevens, T.D., and C. R. Philbrick, "A Bistatic Lidar Receiver to Observe Lower Tropospheric Aerosol Properties," Proceedings of the 18th Annual Conference on Atmospheric Transmission Models, 6-8 June 1995, PL-TR-96-2080, Special Report 278, Phillips Laboratory, Hanscom AFB MA 01731, pg 242, 1996b.

Stevens, Timothy D., PhD Dissertation, Department of Electrical Engineering, Penn State University, 1996.

Verghese, Sachin J., Adam H. Willitsford and C. Russell Philbrick, "Raman Lidar Measurements of Aerosol Distribution and Cloud Properties," Lidar Remote Sensing for Environmental Monitoring VI, edited by Upendra N. Singh, Proc. of SPIE Vol. 5887 H-1, 2005, doi: 10.1117/12.620921

Verghese, Sachin, PhD Dissertation, Department of Electrical Engineering, Penn State University, 2008.

Wyant, Andrea M., David M. Brown, Perry S. Edwards, and C. Russell Philbrick, "Multi-wavelength, multi-angular lidar for aerosol characterization" Laser Radar Technology and Applications XIV, Proc. of SPIE Vol. 7323, (8 pages), 2009, doi: 10.1117/12.818686